Leakage Inductances of Transformers at Arbitrarily Located Windings

Marcin Jaraczewski * and Tadeusz Sobczyk

Faculty of Electrical and Computer Engineering, Cracow University of Technology, 24 Warszawska Street, PL 31-155 Cracow, Poland; pesobczy@cyf-kr.edu.pl
* Correspondence: jaracz@pk.edu.pl; Tel.: +48-12-628-2658

check for
updates

Abstract: The article presents the calculation of the leakage inductance in power transformers. As a rule, the leakage flux in the transformer window is represented by the short-circuit inductance, which affects the short-circuit voltage, and this is a very important factor for power transformers. This inductance reflects the typical windings of power transformers well, but is insufficient for special transformers or in any case of the internal asymmetry of windings. This paper presents a methodology for calculations of the self- and mutual-leakage inductances for windings arbitrarily located in the air window. It is based on the 2D approach for analyzing the stray field in the air zone only, using discrete partial differential operators. That methodology is verified with the finite element method tested on real transformer data.

Keywords: power transformers; winding asymmetry; 2D stray field analysis; 2D discrete partial differential operators; energy-based approach; leakage inductances

1. Introduction

In the long history of research on power transformers, countless books have been published, for example [1–7]. Theoretically, basic construction and operational problems were solved there. In addition to single-phase and three-phase transformers, new types of special power transformers for power system control, power electronics, and electric and traction have been designed. Two approaches are used to analyze the properties of transformers. The first is based on Maxwell's field equations. The second is based on Kirchhoff's equations with mutual-inductances. The field approach is mainly used for transformer design problems, the second for operational problems when the transformer is part of the system. The field approach uses the design data of magnetic circuits and windings, the circuital approach requires relations between the linked fluxes of lumped inductances of the transformer windings and the winding currents. Due to the magnetic non-linearity of the transformer ferromagnetic core, these relations are non-linear, which can only be determined by solving Maxwell's equations [8–15]. Nowadays, software packages allow us to combine the field and the circuit approaches and calculate output values like currents or voltages at transient or steady-states that are interesting for engineers [16]. However, this is costly and time-consuming and seems inappropriate for solving operational problems in systems with power transformers. Therefore, simplified methods for calculating the lumped parameters of a transformer are often used [17–22].

To overcome the difficulties of 2D or 3D non-linear magnetic field computation in the whole transformer magnetic circuit, the relations between linked fluxes ψ_n and currents i_n of elementary

windings, which are necessary for the Kirchhoff's equations of transformers, can be presented in the form:

$$
\begin{bmatrix} \psi_1 \\ \psi_2 \\ \vdots \\ \psi_N \end{bmatrix} = \left\{ \begin{bmatrix} L_{1,1}^{\mu}(\mathbf{i}) & L_{1,2}^{\mu}(\mathbf{i}) & \cdots & L_{1,N}^{\mu}(\mathbf{i}) \\ & L_{2,2}^{\mu}(\mathbf{i}) & \cdots & L_{2,N}^{\mu}(\mathbf{i}) \\ & & \ddots & \vdots \\ (\mathrm{sym}) & & & L_{N,N}^{\mu}(\mathbf{i}) \end{bmatrix} + \begin{bmatrix} L_{1,1}^{\sigma} & L'^{\sigma}_{1,2} & \cdots & L'^{\sigma}_{1,N} \\ & L'^{\sigma}_{2,2} & \cdots & L'^{\sigma}_{2,N} \\ & & \ddots & \vdots \\ (\mathrm{sym}) & & & L'^{\sigma}_{N,N} \end{bmatrix} \right\} \begin{bmatrix} i_1 \\ i_2 \\ \vdots \\ i_N \end{bmatrix} \quad \mathbf{i} = \{i_1, i_1, \ldots, i_N\} \quad (1)
$$

The above two matrices can be calculated separately using a simplified method. The first matrix has inductances, due to fluxes in the core, and the second one results from the leakage field in the transformer windows. Inductances $L_{n,m}^{\mu}(\mathbf{i})$ are non-linear, taking into account the saturation of the ferromagnetic core, and may depend on all winding currents. This matrix can be determined using circuit representation of ferromagnetic core with non-linear lumped parameters, omitting fluxes in the air. The second matrix, containing the leakage inductances, can be found taking into account only the window zone and assuming that $\mu_{Fe} \to \infty$. The leakage inductances $L_{n,m}^{\sigma}$ are constant because the window zone is magnetically linear.

For symmetrically designed power transformers, with magnetic circuits and winding locations sketched in Figure 1, the matrices in (1) take extremely simple forms, which are well known from books and textbooks. Commonly, those matrices are determined by three lumped parameters: Non-linear magnetizing inductance $L_{\mu}(i_{\mu})$ and two leakage inductances of primary L_P^{σ} and secondary winding L_s^{σ}. The inductance $L_{\mu}(i_{\mu})$ represents relation between the linked flux in the limb and the magnetizing current. The sum of leakages inductances determines the short-circuit inductance L_{sc}, and consequently, the short-circuit voltage. It is a very important technical parameter of power transformers. The short-circuit inductance is calculated from the magnetic field in the transformer window with two windings on the same limb, assuming that the ampere-turn compensates and the magnetic permeability of the ferromagnetic core is sufficiently high. The field analysis in the 1D transformer window model provides rather simple formulae for the short circuit inductance. This can be found in books on transformers, and is still recommended for designers. The leakage inductances L_P^{σ} and L_s^{σ} are not calculated, but estimated based on the short circuit inductance [19,20], often just by dividing the short-circuit inductance by 2. This approach is sufficient for symmetrically located windings, when they cover, more or less, the limbs, and the Rogowski factor can correct the length of the magnetic field path in the air. Figure 2a illustrates such a case. Figure 2b shows the position of windings when HV windings are modified, for voltage regulation purposes, by eliminating some numbers of turns in the middle part. Figure 3a presents a case when a short circuit in the HV winding in phase 'A' arise. For the cases 'b' and 'c' leakage inductances cannot be estimated from 1D field analysis.
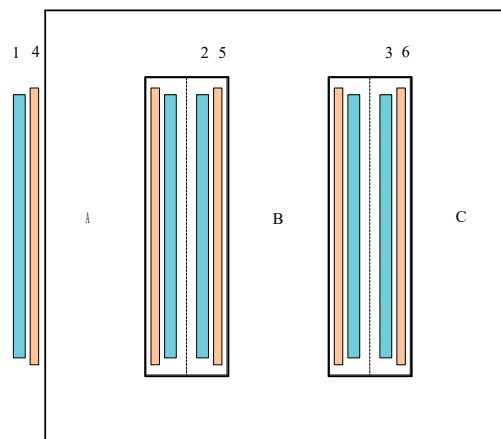

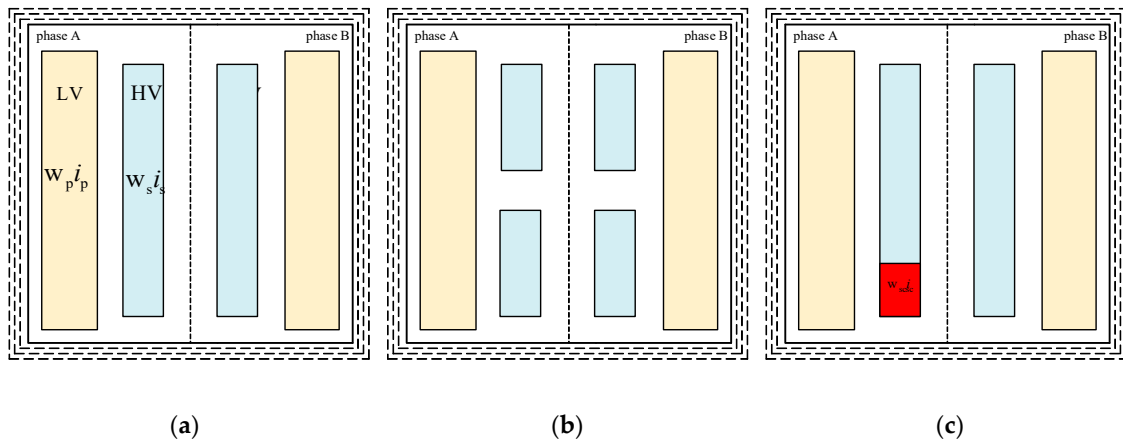**Figure 1.** Locations of three phase transformer windings.

Figure 2. Examples of the location of windings in the air window of three phase transformers: (**a**) Symmetrical; (**b**) at voltage regulation; (**c**) at short circuit of a part of a winding.
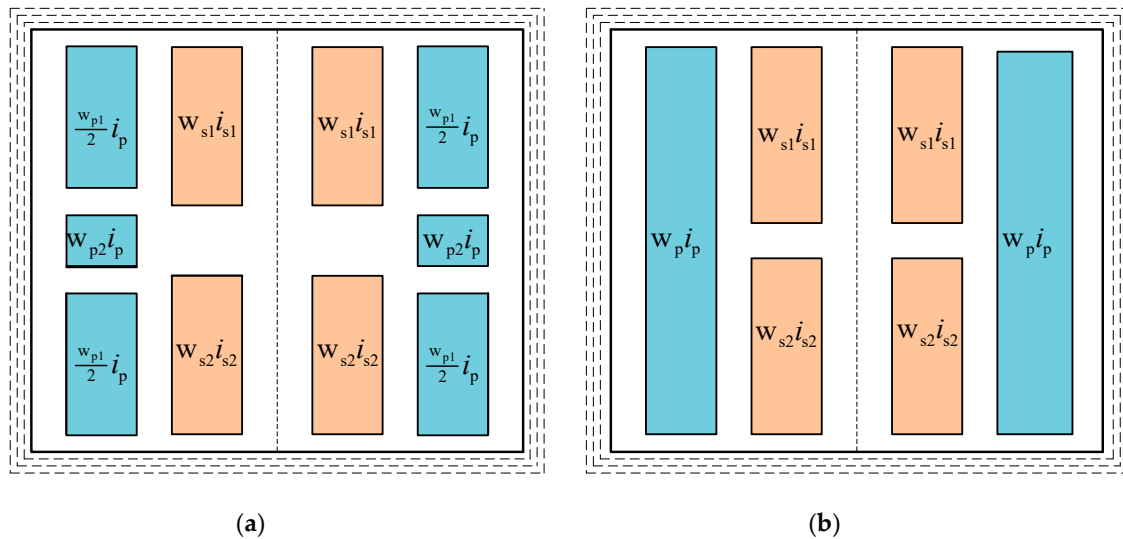

Figure 3. Windings location in rectifier transformers: (**a**) 3/6 phase transformers; (**b**) 3/6 phase transformers for 24 pulses rectifier.

Rectifier transformers for multi-phase voltages and currents [7] can have windings that are much shorter than the limb's height, and the Rogowski factor cannot be applied. Figure 2a shows an example of the location of the windings in the transformer window for Yyd 3/6-phase transformers for 12 pulses rectifiers and Figure 2b for $Y_z$yd 3/12-phase transformers for 24 pulses rectifiers. The position of the windings loses the characteristic symmetry for classic three-phase power transformers, see Figure 1. At least the 2D field is necessary to find leakage inductances.

An analytical solution of the magnetic vector potential in transformer air windows with arbitrarily located balanced pairs of windings is presented in [21]. The zero Neumann boundary conditions can be stated for such cases on the ferromagnetic boundaries, which means that the magnetizing current is omitted. We can then calculate the short circuit inductance for any pair of windings. However, this approach cannot be used to determine the leakage inductances of individual windings and the mutual-inductances caused by the stray field. To find these inductances, 2D or 3D field calculations are typically needed, including the entire magnetic circuit with the ferromagnetic core and the air zone. [11–15,22,23].

This paper presents a 2D numerical approach for determining all leakage inductances $L_{n,m}^{\sigma}$, both self, as well as mutual, for arbitrarily located windings considering the magnetic field in the air window only, when surrounded by ferromagnetic walls with high permeability. Difficulties in

formulating the boundary conditions for the case of one winding in the air window has been omitted based on the results of test calculations using the 2D Finite Element Method (FEM). Ferromagnetic plates with sufficiently high magnetic permeability around the air window have been included for that calculations at zero Dirichlet condition on external boundaries. To fulfill the conditions that were followed for those tests, additional ampere-turns have been added at the boundaries. It allowed us to obtain the magnetic vector potential distribution in the air window area the same as form the FEM method, with sufficiently good accuracy. Self- and mutual-leakage inductances can be calculated using an energy approach. This time, however, each pair of windings is represented by two self-inductances and one mutual-inductance instead of one short-circuit inductance. In this way, it is possible to determine all elements of the leakage induction matrix in equation ((1)). When the elementary windings are connected, constituting the final transformer's windings, the matrix of constraints $\mathbf{C}$ can be defined and the final inductance matrix takes the form,

$$\mathbf{L} = \mathbf{C}^T \cdot (\mathbf{L}_\mu + \mathbf{L}_\sigma) \cdot \mathbf{C} \tag{2}$$

The paper is organized as follows: In the second section, numerical tests are presented, leading to a formulation of boundary conditions on ferromagnetic walls on the air window for unbalanced ampere-turns in the air window. For this purpose, the 2D FEM has been applied. In Section 3, the finite-difference equations have been formulated for magnetic potential in 2D air zone using the Discrete Partial Differential Operators (DPDO), which are presented in Appendix A. Results have been compared to those from FEM, confirming satisfactory accuracy. Section 4 presents energy-based calculations of self- and mutual-inductances, due to fluxes in the air window. The results for two cases: Windings typical location of a three phase power transformers and for short-circuited part of a winding are presented in Section 5. Finally, conclusions are given in Section 6.

2. Calculations of Magnetic Field in the Transformer's Air Window with FEM

To determine the leakage inductance matrix $\mathbf{L}_\sigma$, the self- and mutual-inductances for each pair of windings should be calculated. As an example, a pair of arbitrarily located windings is illustrated in Figure 4.
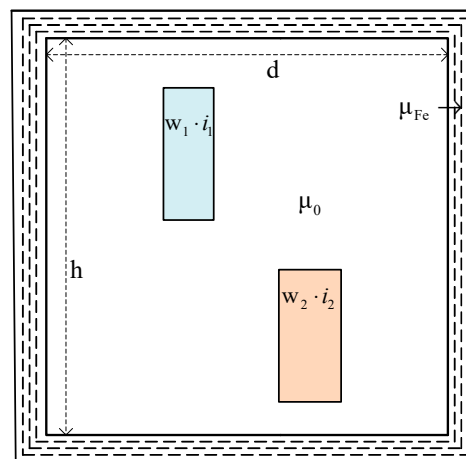

Figure 4. 2D problem for a transformer window with two arbitrarily located windings.

Calculation of self-inductances is not a trivial problem because the magnetic field in the air window zone should be generated by one winding only, omitting a magnetic core. It is not possible to formulate the boundary conditions for the equation of the magnetic potential for such a case, as it

has been explained in [24]. In 2D, the magnetic potential in the air window is described by the partial differential equation of the form:

$$\frac{\partial^2 A(x,y)}{\partial x^2} + \frac{\partial^2 A(x,y)}{\partial y^2} = -\mu_0 (j_1(x,y) + j_2(x,y)) \tag{3}$$

where $A(x,y)$ is the magnetic potential, $j_1(x,y)$ and $j_2(x,y)$ are ampere-turns densities of respective windings. The windings with currents i_1 and i_2 have numbers of turns w_1 and w_2 respectively. Taking into account the ferromagnetic, the zero Dirichlet conditions can be determined on the external circumference of the ferromagnetic core. However, by omitting the ferromagnetic core, i.e., assuming $\mu_{Fe} = \infty$, it is not possible to formulate the boundary conditions only for the air window. The zero Neumann conditions are applicable only in the case of balanced ampere-turns $w_1 \cdot i_1 + w_2 \cdot i_2 = 0$ [23]. To determine the boundary conditions for non-balanced ampere-turns in the transformer window, some numeric test was carried out. The magnetic potential was calculated for the case when only one winding exists in the air window, i.e., $w_2 \cdot i_2 = 0$, but the ferromagnetic walls are included too. The 2D finite elements software has been used here, assuming zero Dirichlet conditions at the outer boundaries of the ferromagnetic core. The permeability of ferromagnetic μ_{Fe} have been rising up to $10\,000 \cdot \mu_0$ in successive calculations. Figure 5 shows the magnetic potential distribution $A(x,y)$ in the air zone only when one winding generates the field at the highest value of magnetic permeability μ_{Fe}.
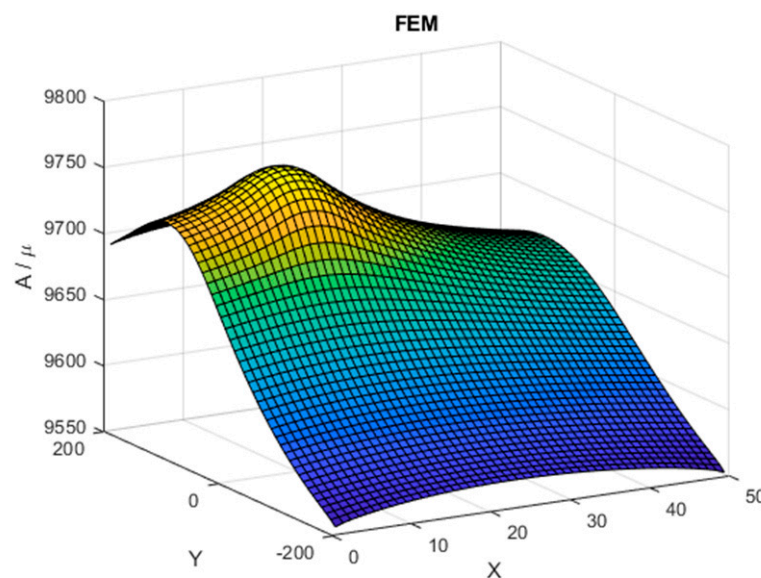

Figure 5. Magnetic potential $A(x,y)/\mu_0$ in the air window was obtained from the finite element method.

Figure 6 presents the components of the magnetic field $H_x(x,y)$ and $H_y(x,y)$ along boundaries of the air window, where

$$H_x(x,y) = \frac{1}{\mu_0} \frac{d}{dy} A(x,y) \quad H_y(x,y) = -\frac{1}{\mu_0} \frac{d}{dx} A(x,y)$$
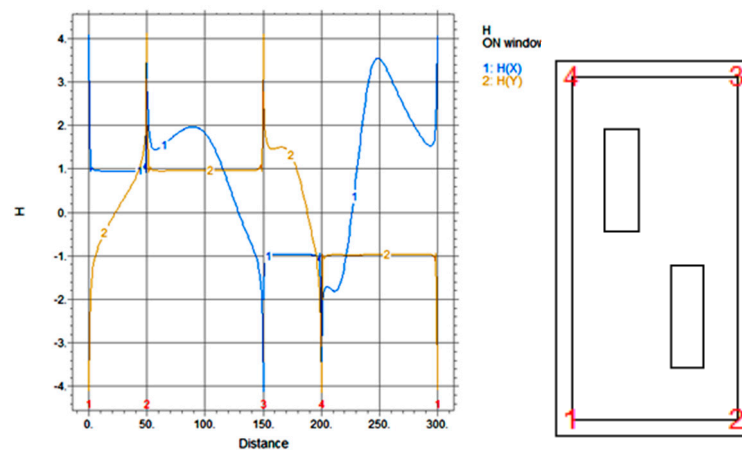
Figure 6. Components of the magnetic field $H_x(x, y)$ and $H_y(x, y)$ along boundaries.

Results of FEM calculations show that the tangential components H_t of a magnetic field on the air window boundaries keep constant values. Its value can be determined from the integral form of the Maxwell equation,

$$\oint_l H_t \mathrm{d}l = \iint_S j(x, y)\mathrm{d}x\mathrm{d}y \tag{4}$$

The curve 'l' is the circumference of the air window and 'S' is the surface limited by this curve. The value of that component equals $H_t = w_1 \cdot i_1 / (2 \cdot (h + d))$ in considered case.

In this paper it is proposed to modify the ampere-turns function in the air window instead of solving the Equation (3) with zero Neumann boundary conditions when omitting $j_2(x, y)$. This modification results in ampere-turns that are now balanced. To eliminate the ferromagnetic core from the computation a general formula for tangential components on both sides of the boundary $H_t^{air} - H_t^{Fe} = 0$ has been changed to $H_t^{air} - 0 = K_z$, where K_z is a surface current in 'z' direction, which equals to the constant component H_t found using FEM

$$K_z = H_t = w_1 \cdot i_1 / (2(h + d)) \tag{5}$$

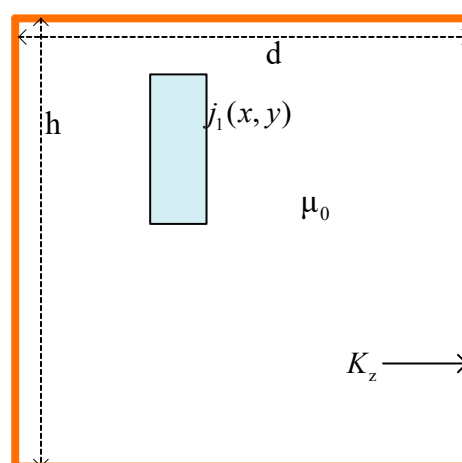That additional surface current is located on the air window boundary, as it is presented in Figure 7.

Figure 7. Additional surface current on the air boundaries.

The exciting function is now balanced and satisfies the relation,

$$\iint\limits_{\substack{0 <x< 2\pi \\ 0 <y< 2\pi}} j_1(x,y)\,\mathrm{d}x\,\mathrm{d}y = \iint\limits_{\substack{0 <x< 2\pi \\ 0 <y< 2\pi}} \nabla \cdot \vec{K}(x,y)\,\mathrm{d}x\,\mathrm{d}y \tag{6}$$

3. Calculations of Magnetic Field in the Transformer Air Window using PDPO

The equation with a modified excitation has the form,

$$\left(\frac{\partial^2 A(x,y)}{\partial x^2} + \frac{\partial^2 A(x,y)}{\partial y^2}\right) = -\mu_0 \cdot \left(j_{\mathrm{mod}}(x,y)\right) \tag{7}$$

where

$$j_{\mathrm{mod}}(x,y) = j_1(x,y) - \frac{\partial K_z(x,y)}{\partial x} - \frac{\partial K_z(x,y)}{\partial y}$$

and can be solved for zero Neumann conditions at all boundaries. The modified excitation is compared to the windings ampere-turn function in Figure 8.
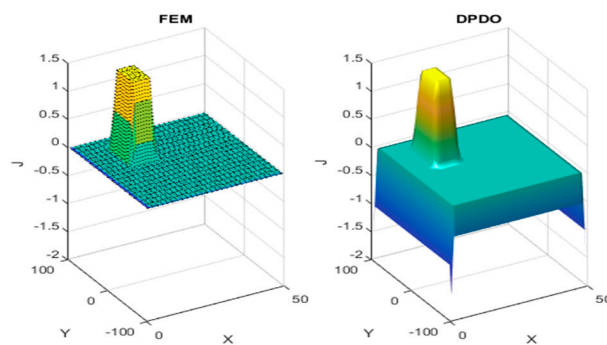

Figure 8. Ampere-turn function $j_1(x,y)$ and the modified excitation $j_{\mathrm{mod}}(x,y)$ for $\mathrm{d}y/\mathrm{d}x = 2$.

The solution of that equation can be predicted in the form of the double Fourier series of cosine functions [24],

$$A(x,y) = \sum_{r=0}^{\infty}\sum_{s=0}^{\infty} A_{r,s} \cdot \left(\cos(r \cdot \pi \cdot \frac{x}{\mathrm{d}}) \cdot \cos(s \cdot \pi \cdot \frac{x}{\mathrm{h}})\right) \text{at } A_{0,0} \equiv 0 \tag{8}$$

The function $j_{\mathrm{mod}}(x,y)$ is rather inconvenient for the Fourier analysis, so to solve Equation (6) a special numerical approach has been applied. To find the magnetic potential the DPDO [25,26] have been developed for the series (8). Full consideration leading to the DPDO are presented in Appendix A. The DPDO have been successfully applied for solving 1D boundary problems [24–26].

The Finite-Difference Equations (FDE) can be rather easily written using DPDO operators, and it takes the form,

$$\mu_0 \cdot \mathbf{D}^{(2)} \cdot \mathbf{A} = -\mathbf{J} \quad \text{where} \quad \mathbf{D}^{(2)} = \left(\mathbf{D}_{\mathrm{xx}}^{(2)} + \mathbf{D}_{\mathrm{yy}}^{(2)}\right) \tag{9}$$

The vectors $\mathbf{A}$ and $\mathbf{J}$ are composed like vectors $\mathbf{z}$ and $\mathbf{g}$ in Appendix A. The matrix $\mathbf{D}^{(2)}$ is singular and has only one eigenvalue equal to zero, so its rank is $((R+1) \cdot (S+1) - 1)$. As it has been mention before the series should satisfy the condition $A_{0,0} = 0$, i.e.,

$$\sum_{n=1}^{R+1}\sum_{m=1}^{S+1} A_{n,m} = 0 \tag{10}$$

It is, in fact, the constraint equation for the elements of the vector **A**, which can be expressed in the form:

$$\mathbf{A} = \begin{bmatrix} A_{1,1} \\ A_{1,2} \\ \vdots \\ A_{R+1,S+1} \end{bmatrix} = \begin{bmatrix} -1 & \cdots & -1 \\ 1 & & \\ & \ddots & \\ & & 1 \end{bmatrix} \begin{bmatrix} A_{1,2} \\ \vdots \\ A_{R+1,S+1} \end{bmatrix} = \mathbf{C} \cdot \mathbf{A_C} \tag{11}$$

where **C** is the constraint matrix. Finally, the FDEs can be written in the form,

$$\mu_0 \cdot \left(\mathbf{C}^T \cdot \mathbf{D}^{(2)} \cdot \mathbf{C} \right) \cdot \mathbf{A_C} = -\mathbf{C}^T \cdot \mathbf{J} \tag{12}$$

The matrix $\mathbf{C}^T \cdot \mathbf{D}^{(2)} \cdot \mathbf{C} = \mathbf{D}_C^{(2)}$ is non-singular, and the new FDEs (12) have a unique solution.

The algorithm for solving the FDE (12) has been prepared in MATLAB, and the resulting magnetic potential distribution in the air window area is presented in Figure 9, denoted as DPDO. These results are compared to the results of FEM with a reduced mean value to zero.
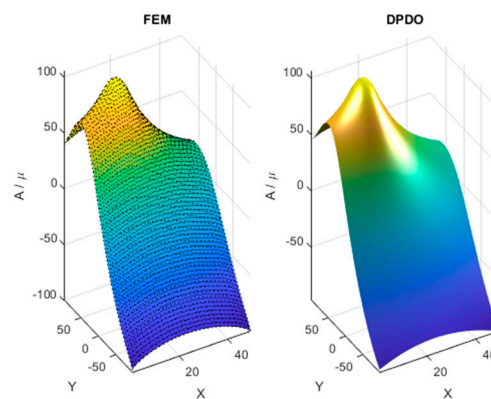

Figure 9. Magnetic potential $A(x,y)/\mu$ in the air window obtained using the Finite Element Method (FEM) and Discrete Partial Differential Operators (DPDO).

The magnetic field distribution,

$$H(x,y) = \sqrt{(H_x(x,y))^2 + (H_y(x,y))^2} \tag{13}$$

has been determined based on $A(x,y)$. The first order DPDO has been used for that. The results, both of FEM and DPDO, are shown in Figure 10.
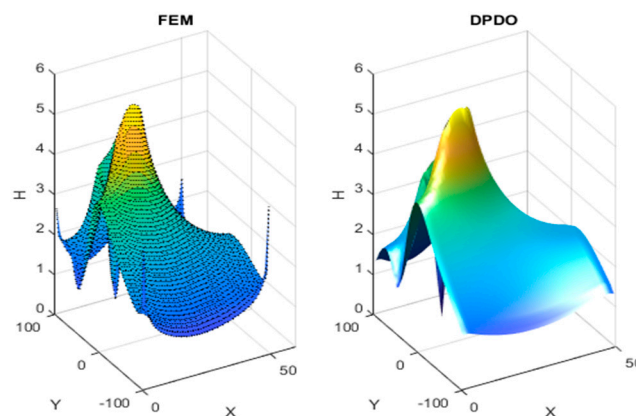

Figure 10. Magnetic field $H(x,y)$ in the air window obtained with FEM and DPDO.

The differences between solutions of magnetic field distributions are presented in Figure 11 and seem to be sufficiently small.
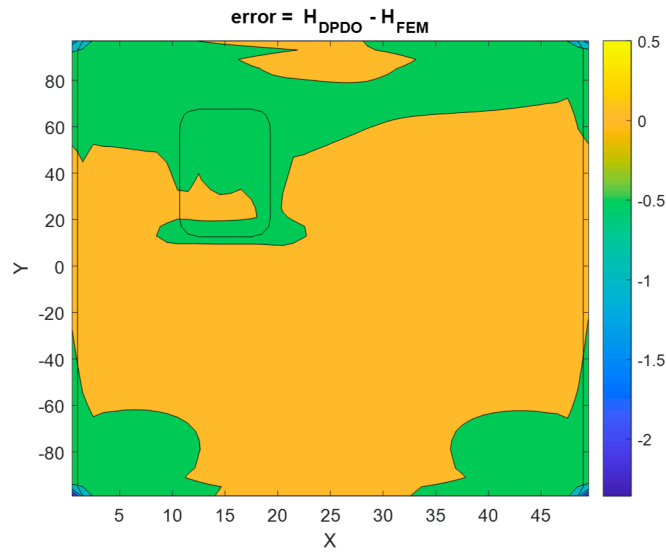

Figure 11. Difference between magnetic field $H(x, y)$ resulting from DPDO and FEM.

and the solution can be predicted as the Fourier series (7). Application of the DPDO leads to the required solution.

4. Co-Energy Based Calculations of Self- and Mutual-Leakage Inductances

The inductances $L_{n,n}^{\sigma}$, $L_{m,m}^{\sigma}$, and $L_{n,m}^{\sigma}$ in the Formula (1) can be calculated based on field distribution in the air window, obtained with application of the second order DPDOs presented in Appendix A. Two formulae of magnetic co-energy stored in the air can be used here. The first one determines co-energy from the distribution of the magnetic field:

$$E_{co} = \frac{1}{2} \iiint_V (\vec{B} \cdot \vec{H}) \, dV \tag{14}$$

and the second is based on lumped inductances of coils,

$$E_{co} = \frac{1}{2} L_{n,n}^{\sigma} \cdot (i_n)^2 + \frac{1}{2} L_{m,m}^{\sigma} \cdot (i_m)^2 + L_{n,m}^{\sigma} \cdot i_n \cdot i_m \tag{15}$$

Inductances can be calculated in three steps:

- Calculate inductance $L_{n,n}^{\sigma}$ from the co-energy $E_{co,n}$ at $i_n = I_n$ and $i_m = 0$,

$$E_{co,n} = \frac{1}{2} L_{n,n}^{\sigma} \cdot (I_n)^2 \tag{16}$$

- Calculate inductance $L_{m,m}^{\sigma}$ from the co-energy $E_{co,m}$ at $i_n = 0$ and $i_m = I_m$,

$$E_{co,m} = \frac{1}{2} L_{m,m}^{\sigma} \cdot (I_m)^2 \tag{17}$$

- Calculate inductance $L_{m,m}^{\sigma}$ from the co-energy $E_{co,nm}$ at $i_n = I_n$ and $i_m = I_m$,

$$E_{co} - E_{co,n} - E_{co,m} = L_{m,m}^{\sigma} \cdot I_n \cdot I_m \tag{18}$$

In 2D the formula of the co-energy takes the form,

$$E_{\text{co}} = \frac{1}{2}\mu_0 \cdot l_{eq} \cdot \int_0^h \int_0^d \left((H_x(x,y))^2 + (H_y(x,y))^2 \right) dxdy \tag{19}$$

where l_{eq} is an equivalent length of the air window in z-direction, usually it is the circumference taken in the middle of the air window.

5. Results of Teste Calculations

5.1. Test 1

As the first test, the leakage inductance matrix $\mathbf{L}_\sigma$ of a typical power transformer has been determined. The transformer is shown schematically in Figure 1. The inductance matrix can be predicted in the form

$$\mathbf{L}_\sigma = \begin{bmatrix} L_{1,1}^\sigma & L_{1,2}^\sigma & 0 & L_{1,4}^\sigma & L_{1,5}^\sigma & 0 \\ & L_{2,2}^\sigma & L_{2,3}^\sigma & L_{2,4}^\sigma & L_{2,5}^\sigma & L_{2,6}^\sigma \\ & & L_{3,3}^\sigma & 0 & L_{3,5}^\sigma & L_{3,6}^\sigma \\ & & & L_{4,4}^\sigma & L_{4,5}^\sigma & 0 \\ & (\text{sym}) & & & L_{5,5}^\sigma & L_{5,6}^\sigma \\ & & & & & L_{6,6}^\sigma \end{bmatrix}$$

Design data, more or less related to a power transformer of about 60MVA, 110/60kV, Yd11 have been used for calculations. Its air window and the winding locations are shown in Figure 12, keeping the proportions. The following data are used for computations: Air window dimensions $h = 1750$ mm, $d = 480$ mm, diameter of limbs $d_{\text{limb}} = 580$mm. The equivalent length of widows in z-direction equals to circumference of a circle of a diameter $l_{eq} = p \cdot (580 + 480)$mm. The winding's dimensions are: HV$-h_1 = 1550$ mm, $d_1 = 70$ mm, LV-$h_2 = 1650$ mm, $d_2 = 50$ mm and the distance between HV and LV windings is $\delta = 30$mm. Numbers of turns are: HV–720 and LV–240.
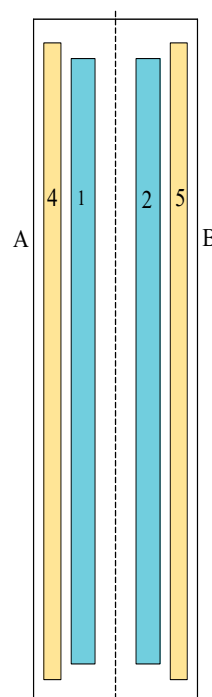

Figure 12. Air window with windings.

The magnetic vector potential in the air window has been determined by solving equation (12) using the second order DPDO, presented in Appendix A. The modified ampere-turn functions have been determined for individual cases. An exemplary winding '1' is presented in Figure 13. The magnetic field distribution in the air window has been obtained using the first order DPDO. The discretization mesh, with $\Delta x = 10$ mm and $\Delta y = 50$ mm has been chosen, i.e., the number of points in x' direction is 49 and in y direction is 36, which leads to 1764 points in the whole area. The leakage inductances have been obtained from equalities (14)–(16) for an arbitrary value of currents.
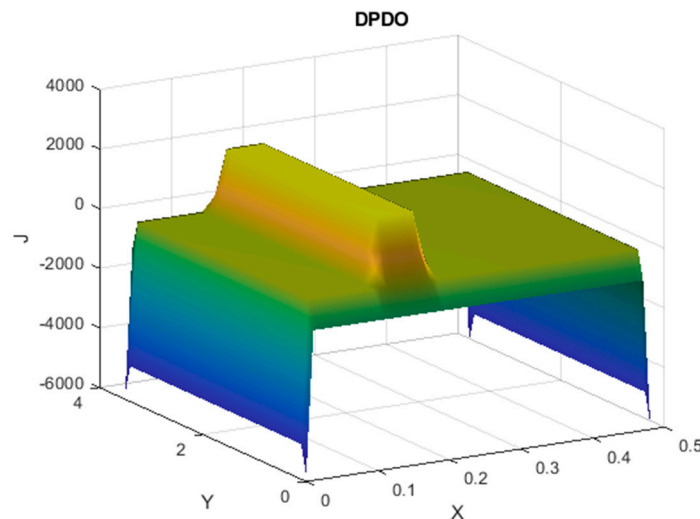

Figure 13. Modified ampere-turn function for winding '1'.

Figure 14 presents distributions of magnetic potential $A(x, y)$ and magnetic field $H(x, y)$ in the air window obtained from FEM and the DPDO.
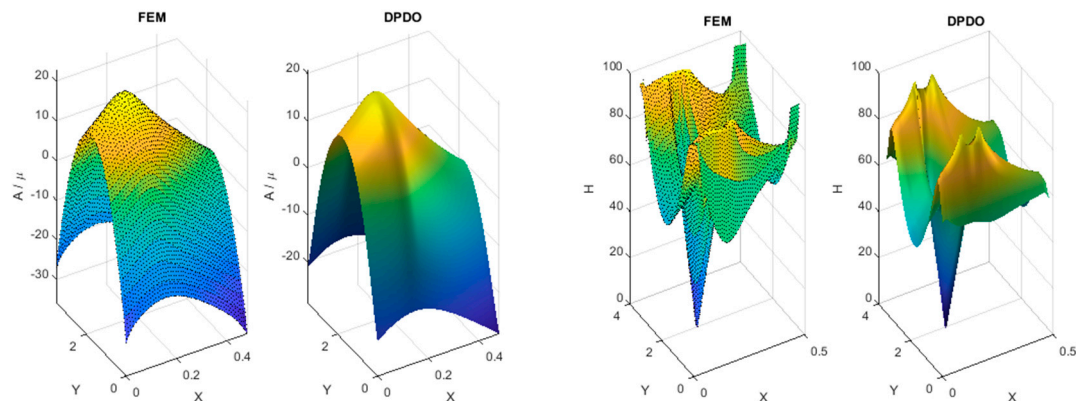

Figure 14. Distributions of magnetic potential $A(x, y)$ and magnetic field $H(x, y)$ in the air zone.

The components of magnetic field $H_x(x, y)$ and $H_y(x, y)$ are shown in Figure 15. The value of $H_x(x)$ on the boundaries in direction x is constant and equals $H_x = \pm 50 A/m$ and $H_y(y)$ on the boundaries in direction y is constant also and equals $H_y = \pm 50 A/m$.
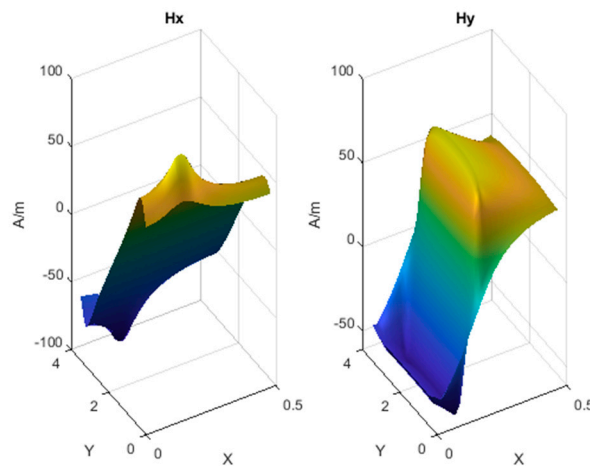
Figure 15. Components $H_x(x, y)$ and $H_y(x, y)$.

The values of leakage inductances have been calculated using relations (14)–(16) for the number of turns of HV winding '1'. The inductance values are presented in the matrix below. The symmetry of windings has been taken into account, which is reflected in matrix structure.

$$
\mathbf{L}_\sigma =
\begin{bmatrix}
203.06 & 93.21 & 0 & 153.41 & 30.07 & 0 \\
 & 203.06 & 93.21 & 31.10 & 153.41 & 30.07 \\
 & & 203.06 & 0 & 31.10 & 153.41 \\
 & & & 195.95 & -26.74 & 0 \\
 & (sym) & & & 195.95 & -26.74 \\
 & & & & & 195.95
\end{bmatrix} \cdot 10^{-3} \mathrm{H}
$$

The short circuit inductance, when accounting for the couplings between the windings on the same limb only, equals $L_{sc} = 82.19$ mH. The same matrix calculated from expressions presented in [24], obtained in 1D approach, has the form,

$$
\mathbf{L}_\sigma =
\begin{bmatrix}
134.20 & 30.97 & 0 & 92.91 & -24.78 & 0 \\
 & 134.20 & 30.97 & -24.78 & 92.91 & -24.78 \\
 & & 134.20 & 0 & -24.78 & 92.91 \\
 & & & 138.33 & -80.52 & 0 \\
 & (sym) & & & 138.33 & -80.52 \\
 & & & & & 138.33
\end{bmatrix} \cdot 10^{-3} \mathrm{H}
$$

The corresponding short circuit impedance equals $L_{sc} = 86.72$ mH. The differences between those matrices seem to be rather high, but the short circuit inductances are almost equal.

5.2. Test 2

For the second test, the leakage inductance matrix has been determined when the short circuit of a part of HV winding occurs, as it is presented in Figure 16. The same data as for Test 1 have been assumed, but 20% of HV winding is short circuited. For that test, the other windings have been omitted. For that case, the leakage inductance matrix takes the form,

$$
\mathbf{L}_\sigma =
\begin{bmatrix}
L_{1,1}^\sigma & L_{1,2}^\sigma & L_{1,sc}^\sigma \\
 & L_{2,2}^\sigma & L_{sc,2}^\sigma \\
(sym) & & L_{sc}^\sigma
\end{bmatrix}
$$

and values of respective inductances are,

$$\mathbf{L}_\sigma = \begin{bmatrix} 229.84 & 47.31 & -44.22 \\ & 21.78 & 5.38 \\ (\text{sym}) & & 66.80 \end{bmatrix}$$

These inductances cannot be found from a 1D approach. To confirm it, the magnetic potential distribution in the short circuit coil case is shown in Figure 17.
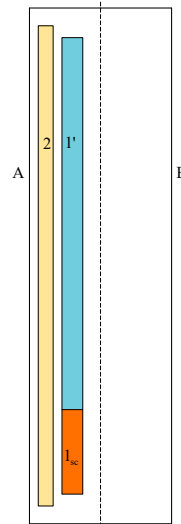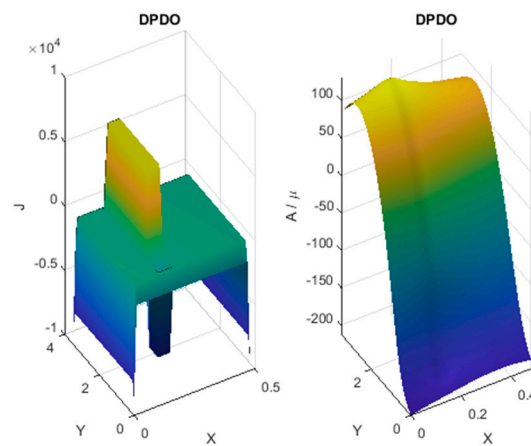

Figure 16. Windings with short circuit.

Figure 17. The current density and magnetic potential distribution for short circuited winding '1'.

6. Conclusions

This paper presented a method for calculations of self- and mutual-leakage inductances of power transformer windings with arbitrary winding locations in the air windows. It was possible to obtain inductance values based on 2D calculations of the magnetic field only in the air zone, using discrete partial differential operators for 2D periodic functions. The boundary conditions which allowed for the elimination of the transformer ferromagnetic core were determined based on the test calculations of the magnetic field distribution using FEM that included a transformer core of sufficiently high permeability. It followed that the surface current should be located on the boundaries.

To find the solution predicted in the air zone, the discrete partial differential operators of the first- and the second orders have been developed and presented in Appendix A. They allowed us to easily create the finite-difference equations determining the 2D magnetic vector potential distribution in the air window, and consequently, the distribution of the magnetic field strength. The results are sufficiently accurate comparing to FEM.

The energy-based method has been successfully used to calculate the leakage inductances, both the self- and mutual-inductances. The matrix of such inductances has been calculated for the design data of a real three-phase power transformer. For a case when a part of one winding on one limb is short circuited, the inductances have also been calculated.

Appendix A

Discrete Differential Operators for Double Cosine Fourier Series

Discrete Partial Differential Operators (DPDOs) are developed for the two-variable periodic function $z(x, y)$, which is defined in the area $0 < x < 2\pi, 0 < y < 2\pi$, and can be expanded in the Fourier series with a limited number of terms,

$$z(x, y) = \sum_{r=0}^{R} \sum_{s=0}^{S} Z_{r,s} \cdot (\cos(r \cdot x/2) \cdot \cos(s \cdot y/2)) \tag{A1}$$

Firstly, the unique relations between the function values and the Fourier coefficients can be found. To determine that relation the set of $((R + 1) \times (S + 1))$ points uniformly distributed in the area has been chosen, as shown in Figure A1.

$$
\begin{array}{ll}
x_1 = \Delta x/2 & y_1 = \Delta y/2 \\
x_2 = \Delta x/2 + \Delta x & y_2 = \Delta y/2 + \Delta y \\
x_3 = \Delta x/2 + 2\Delta x & y_3 = \Delta y/2 + 2\Delta y \\
\quad\vdots & \quad\vdots \\
x_{R+1} = \pi - \Delta x/2 & y_{S+1} = \pi - \Delta y/2
\end{array}
\tag{A2}
$$

where $\Delta x = \pi/(R + 1), \Delta y = \pi/(S + 1)$.

Proper ordering of the point set $\{x_n, y_m\}$ allows writing relations between the set of function values $\{z_{n,m}\}$ and the set of Fourier coefficients $\{Z_{r,s}\}$ in the form

$$\mathbf{z} = \mathbf{T} \cdot \mathbf{Z} \tag{A3}$$

where $\mathbf{z}$ is a vector of the function values $\{z_{n,m}\}$, ordered, as follows,

$$\mathbf{z} = \begin{bmatrix} \mathbf{z}_1 & \mathbf{z}_2 & \cdots & \mathbf{z}_{R+1} \end{bmatrix}^T \text{ where } \mathbf{z}_n = \begin{bmatrix} z_{n,1} & z_{n,2} & \cdots & z_{n,S+1} \end{bmatrix}$$
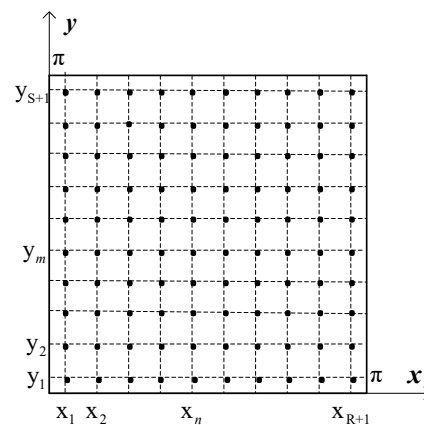
Figure A1. Discretization of the function's area

The vector **Z** contains the Fourier coefficients of the series (A1),

$$\mathbf{Z} = \begin{bmatrix} \mathbf{Z}_0 & \mathbf{Z}_1 & \cdots & \mathbf{Z}_R \end{bmatrix}^T \quad \text{where} \mathbf{Z}_r = \begin{bmatrix} Z_{r,0} & Z_{r,1} & \cdots & Z_{r,S} \end{bmatrix}$$

The **T** hyper-matrix has the form,

$$\mathbf{T} = \begin{bmatrix} \cos(0 \cdot x_1) \cdot \mathbf{B} & \cos(1 \cdot x_1) \cdot \mathbf{B} & \cdots & \cos(R \cdot x_1) \cdot \mathbf{B} \\ \cos(0 \cdot x_2) \cdot \mathbf{B} & \cos(1 \cdot x_2) \cdot \mathbf{B} & \cdots & \cos(R \cdot x_2) \cdot \mathbf{B} \\ \vdots & \vdots & \vdots & \vdots \\ \cos(0 \cdot x_{R+1}) \cdot \mathbf{B} & \cos(1 \cdot x_{R+1}) \cdot \mathbf{B} & \cdots & \cos(R \cdot x_{R+1}) \cdot \mathbf{B} \end{bmatrix} \tag{A4}$$

The **B** matrix is square and has dimension $((S+1) \times (S+1))$. It takes the form,

$$\mathbf{B} = \begin{bmatrix} \cos(0 \cdot y_1) & \cos(1 \cdot y_1) & \cdots & \cos(S \cdot y_1) \\ \cos(0 \cdot y_2) & \cos(1 \cdot y_2) & \cdots & \cos(S \cdot y_2) \\ \vdots & \vdots & \vdots & \vdots \\ \cos(0 \cdot y_{S+1}) & \cos(1 \cdot y_{S+1}) & \cdots & \cos(S \cdot y_{S+1}) \end{bmatrix} \tag{A5}$$

The **T** matrix has dimension $((R+1) \times (S+1))$. Its inverse matrix can be calculated from the formula,

$$\mathbf{T}^{-1} = \left(\mathbf{T}^T \cdot \mathbf{T} \right)^{-1} \cdot \mathbf{T}^T$$

The $(\mathbf{T}^T \cdot \mathbf{T})$ matrix is a diagonal of the form,

$$\mathbf{T}^T \cdot \mathbf{T} = ((R+1) \cdot (S+1)) \cdot \text{diag} \begin{bmatrix} \mathbf{C}_S & (1/2) \cdot \mathbf{C}_S & \cdots & (1/2) \cdot \mathbf{C}_S \end{bmatrix} = \mathbf{CC}_S = \text{diag} \begin{bmatrix} 1 & 1/2 & \cdots & 1/2 \end{bmatrix}$$

The inverse matrix $\mathbf{T}^{-1}$ can be determined from the relation,

$$\mathbf{C}^{-1} = \left(\mathbf{T}^T \cdot \mathbf{T} \right)^{-1} = \mathbf{T}^{-1} \cdot \left(\mathbf{T}^T \right)^{-1}$$

Obtaining,

$$\mathbf{T}^{-1} = \mathbf{C}^{-1} \cdot \mathbf{T}^T = \tfrac{1}{(R+1) \cdot (S+1)} \cdot \text{diag} \begin{bmatrix} \mathbf{C}_S^{-1} & 2 \cdot \mathbf{C}_S^{-1} & \cdots & 2 \cdot \mathbf{C}_S^{-1} \end{bmatrix} \cdot \mathbf{T}^T$$
$$\mathbf{C}_S^{-1} = \text{diag} \begin{bmatrix} 1 & 2 & \cdots & 2 \end{bmatrix}$$

Therefore, the inverse relation to (A3) can be written as,

$$\mathbf{Z} = \frac{1}{(R+1)\cdot(S+1)} \cdot \text{diag}\begin{bmatrix} \mathbf{C_S}^{-1} & 2\cdot\mathbf{C_S}^{-1} & \cdots & 2\cdot\mathbf{C_S}^{-1} \end{bmatrix} \cdot \mathbf{T}^\mathsf{T} \cdot \mathbf{z} \qquad (A6)$$

If the first partial derivatives exist, they have the Fourier series forms,

$$z'_\text{x}(x,y) = \sum_{r=0}^{R}\sum_{s=0}^{S}(-r\cdot Z_{r,s})\cdot(\sin(r\cdot x)\cdot\cos(s\cdot y)) = \sum_{r=0}^{R}\sum_{s=0}^{S}(Z'_{\text{x},r,s})\cdot(\sin(r\cdot x)\cdot\cos(s\cdot y)) \quad (A7)$$

$$z'_\text{y}(x,y) = \sum_{r=0}^{R}\sum_{s=0}^{S}(-s\cdot Z_{r,s})\cdot(\cos(r\cdot x)\cdot\sin(s\cdot y)) = \sum_{r=0}^{R}\sum_{s=0}^{S}(Z'_{\text{y},r,s})\cdot(\cos(r\cdot x)\cdot\sin(s\cdot y)) \quad (A8)$$

It can be used to find a relation between the Fourier coefficients of the series (A1) and (A7), (A8). They can be written in the forms,

$$\mathbf{Z'}_\text{x} = \mathbf{R}_\text{x}\cdot\mathbf{Z} \text{ and } \mathbf{Z'}_\text{y} = \mathbf{R}_\text{y}\cdot\mathbf{Z} \qquad (A9)$$

$\mathbf{Z'}_\text{x}$ and $\mathbf{Z'}_\text{y}$ are vectors of the Fourier coefficients of the respective series of partial derivatives (A7), (A8), ordered analogously,

$$\mathbf{Z'}_\text{x} = \begin{bmatrix} \mathbf{Z'}_{\text{x},0} & \mathbf{Z'}_{\text{x},1} & \cdots & \mathbf{Z'}_{\text{x},R} \end{bmatrix}^T \text{ where } \mathbf{Z'}_{\text{x},r} = \begin{bmatrix} Z'_{\text{x},r,0} & Z'_{\text{x},r,1} & \cdots & Z'_{\text{x},r,S} \end{bmatrix}$$

and

$$\mathbf{Z'}_\text{y} = \begin{bmatrix} \mathbf{Z'}_{\text{y},0} & \mathbf{Z'}_{\text{y},1} & \cdots & \mathbf{Z'}_{\text{y},R} \end{bmatrix}^T \text{ where } \mathbf{Z'}_{\text{y},r} = \begin{bmatrix} Z'_{\text{y},r,0} & Z'_{\text{y},r,1} & \cdots & Z'_{\text{y},r,S} \end{bmatrix}$$

The matrices $\mathbf{R}_\text{x}$ and $\mathbf{R}_\text{y}$ stand for the differential operators of a 2D periodic function in the frequency domain with respect to 'x' and 'y'. They are diagonal. The matrix $\mathbf{R}_\text{x}$ is constituted by $(R + 1)$ diagonal $\mathbf{R}_{\text{x},r}$ matrices,

$$\mathbf{R}_\text{x} = \text{diag}\begin{bmatrix} \mathbf{R}_{\text{x},0} & \mathbf{R}_{\text{x},1} & \cdots & \mathbf{R}_{\text{x},R} \end{bmatrix}$$

Each of them is diagonal too and has dimension $((S+1)\times(S+1))$ and takes the form,

$$\mathbf{R}_{\text{x},r} = -r\cdot\text{diag}\begin{bmatrix} 1 & 1 & \cdots & 1 \end{bmatrix}$$

The matrix $\mathbf{R}_\text{y}$ is also constituted by $(R + 1)$ matrices $\mathbf{R}_{\text{y},r}$,

$$\mathbf{R}_\text{y} = \text{diag}\begin{bmatrix} \mathbf{R}_{\text{y},0} & \mathbf{R}_{\text{y},1} & \cdots & \mathbf{R}_{\text{y},R} \end{bmatrix}$$

Each matrix $\mathbf{R}_{\text{y},r}$ is diagonal too and have $(S + 1)$ elements,

$$\mathbf{R}_{\text{y},r} = -\text{diag}\begin{bmatrix} 0 & 1 & \cdots & S \end{bmatrix}$$

Analogous to (A3), using the same notations, the relations,

$$\mathbf{Z'}_\text{x} = \mathbf{T}_\text{x}\cdot\mathbf{Z'}_\text{x} \text{ and } \mathbf{z'}_\text{y} = \mathbf{T}_\text{y}\cdot\mathbf{Z'}_\text{y} \qquad (A10)$$

can be created. The matrices $\mathbf{T}_x$ and $\mathbf{T}_y$ have the forms,

$$\mathbf{T}_x = \begin{bmatrix} \sin(0 \cdot x_1) \cdot \mathbf{B} & \sin(1 \cdot x_1) \cdot \mathbf{B} & \cdots & \sin(R \cdot x_1) \cdot \mathbf{B} \\ \sin(0 \cdot x_2) \cdot \mathbf{B} & \sin(1 \cdot x_2) \cdot \mathbf{B} & \cdots & \sin(R \cdot x_2) \cdot \mathbf{B} \\ \vdots & \vdots & \vdots & \vdots \\ \sin(0 \cdot x_{R+1}) \cdot \mathbf{B} & \sin(1 \cdot x_{R+1}) \cdot \mathbf{B} & \cdots & \sin(R \cdot x_{R+1}) \cdot \mathbf{B} \end{bmatrix} \tag{A11}$$

$$\mathbf{T}_y = \begin{bmatrix} \cos(0 \cdot x_1) \cdot \mathbf{B}_y & \cos(1 \cdot x_1) \cdot \mathbf{B}_y & \cdots & \cos(R \cdot x_1) \cdot \mathbf{B}_y \\ \cos(0 \cdot x_2) \cdot \mathbf{B}_y & \cos(1 \cdot x_2) \cdot \mathbf{B}_y & \cdots & \cos(R \cdot x_2) \cdot \mathbf{B}_y \\ \vdots & \vdots & \vdots & \vdots \\ \cos(0 \cdot x_{R+1}) \cdot \mathbf{B}_y & \cos(1 \cdot x_{R+1}) \cdot \mathbf{B}_y & \cdots & \cos(R \cdot x_{R+1}) \cdot \mathbf{B}_y \end{bmatrix} \tag{A12}$$

The matrix $\mathbf{B}_y$ has the form,

$$\mathbf{B}_y = \begin{bmatrix} \sin(0 \cdot y_1) & \sin(1 \cdot y_1) & \cdots & \sin(S \cdot y_1) \\ \sin(0 \cdot y_2) & \sin(1 \cdot y_2) & \cdots & \sin(S \cdot y_2) \\ \vdots & \vdots & \vdots & \vdots \\ \sin(0 \cdot y_{S+1}) & \sin(1 \cdot y_{S+1}) & \cdots & \sin(S \cdot y_{S+1}) \end{bmatrix} \tag{A13}$$

Having combined the relations (A3) and (A10), the following equations can be written,

$$(\mathbf{T}_x \cdot \mathbf{Z'}_x) = \left(\mathbf{T}_x \cdot \mathbf{R}_x \cdot \mathbf{T}^{-1}\right) \cdot (\mathbf{T} \cdot \mathbf{Z})$$
$$(\mathbf{T}_y \cdot \mathbf{Z'}_y) = \left(\mathbf{T}_y \cdot \mathbf{R}_y \cdot \mathbf{T}^{-1}\right) \cdot (\mathbf{T} \cdot \mathbf{Z})$$

These lead to relations,

$$\mathbf{Z'}_x = \mathbf{D}_x^{(1)} \cdot \mathbf{z} \quad \mathbf{Z'}_y = \mathbf{D}_y^{(1)} \cdot \mathbf{z} \tag{A14}$$

The matrices $\mathbf{D}_x^{(1)}$ and $\mathbf{D}_y^{(1)}$ are the sought first order discrete partial-differential operators,

$$\mathbf{D}_x^{(1)} = \mathbf{T}_x \cdot \mathbf{R}_x^{(1)} \cdot \mathbf{T}^{\mathrm{T}} \quad \mathbf{D}_y^{(1)} = \mathbf{T}_y \cdot \mathbf{R}_y^{(1)} \cdot \mathbf{T}^{\mathrm{T}} \tag{A15}$$

where

$$\mathbf{R}_x^{(1)} = \mathbf{R}_x \cdot \mathbf{C}^{-1} = \frac{1}{(R+1) \cdot (S+1)} \mathrm{diag}\begin{bmatrix} 0 & \mathbf{R}_{x,1}^{(1)} & \cdots & \mathbf{R}_{x,R}^{(1)} \end{bmatrix} \mathbf{R}_{x,r}^{(1)} = -r \cdot \mathrm{diag}\begin{bmatrix} 2 & 4 & \cdots & 4 \end{bmatrix}$$

$$\mathbf{R}_y^{(1)} = \mathbf{R}_y \cdot \mathbf{C}^{-1} = \frac{1}{(R+1) \cdot (S+1)} \mathrm{diag}\begin{bmatrix} \mathbf{R}_{y,S}^{(1)} & 2 \cdot \mathbf{R}_{y,S}^{(1)} & \cdots & 2 \cdot \mathbf{R}_{y,S}^{(1)} \end{bmatrix}$$

$$\mathbf{R}_{y,S}^{(1)} = -\mathrm{diag}\begin{bmatrix} 0 & 2 \cdot 1 & \cdots & 2 \cdot S \end{bmatrix}$$

The matrices $\mathbf{R}_x^{(1)}$ and $\mathbf{R}_y^{(1)}$ are singular.
The second partial derivatives have the Fourier series forms,

$$z''_{xx}(x,y) = \sum_{r=0}^{R} \sum_{s=0}^{S} (-r^2 \cdot Z_{r,s}) \cdot (\cos(r \cdot x) \cdot \cos(s \cdot y)) = \sum_{r=0}^{R} \sum_{s=0}^{S} (Z''_{xx,r,s}) \cdot (\cos(r \cdot x) \cdot \cos(s \cdot y)) \tag{A16}$$

$$z''_{yy}(x,y) = \sum_{r=0}^{R} \sum_{s=0}^{S} (-s^2 \cdot Z_{r,s}) \cdot (\cos(r \cdot x) \cdot \cos(s \cdot y)) = \sum_{r=0}^{R} \sum_{s=0}^{S} (Z''_{yy,r,s}) \cdot (\cos(r \cdot x) \cdot \cos(s \cdot y)) \tag{A17}$$

$$z''_{xy}(x,y) = \sum_{r=0}^{R} \sum_{s=0}^{S} (r \cdot s \cdot Z_{r,s}) \cdot (\sin(r \cdot x) \cdot \sin(s \cdot y)) = \sum_{r=0}^{R} \sum_{s=0}^{S} (Z''_{xy,r,s}) \cdot (\sin(r \cdot x) \cdot \sin(s \cdot y)) \tag{A18}$$

The relation between the Fourier coefficients of the series (A1) and (A16)–(A18) can be written in the forms,

$$\mathbf{Z}''_{xx} = \mathbf{R}_{xx} \cdot \mathbf{Z}\quad \mathbf{Z}'_{yy} = \mathbf{R}_{yy} \cdot \mathbf{Z}\quad \mathbf{Z}''_{xy} = \mathbf{R}_{xy} \cdot \mathbf{Z} \tag{A19}$$

where $\mathbf{Z}''_{xx}$, $\mathbf{Z}''_{yy}$ and $\mathbf{Z}''_{xy}$ are vectors of the Fourier coefficients of the respective series of the second partial derivatives (A16)–(A18), ordered analogously as it has been used in first derivatives. The matrices $\mathbf{R}_{xx}$, $\mathbf{R}_{yy}$ and $\mathbf{R}_{xy}$ have the following forms. The matrix $\mathbf{R}_{xx}$ is constituted by $(R + 1)$ diagonal $\mathbf{R}_{xx,n}$ matrices,

$$\mathbf{R}_{xx} = \text{diag}\begin{bmatrix} \mathbf{R}_{xx,0} & \mathbf{R}_{xx,1} & \cdots & \mathbf{R}_{xx,R} \end{bmatrix}$$

Each of them is diagonal too and has dimension $((S + 1) \times (S + 1))$ and takes the form,

$$\mathbf{R}_{x,r} = -r^2 \cdot \text{diag}\begin{bmatrix} 1 & 1 & \cdots & 1 \end{bmatrix}$$

The matrix $\mathbf{R}_{yy}$ is also constituted by $(R + 1)$ matrices $\mathbf{R}_{yy,r}$,

$$\mathbf{R}_{yy} = \text{diag}\begin{bmatrix} \mathbf{R}_{yy,0} & \mathbf{R}_{yy,1} & \cdots & \mathbf{R}_{yy,R} \end{bmatrix}$$

Each matrix $\mathbf{R}_{yy,r}$ is diagonal too and has $(S + 1)$ elements,

$$\mathbf{R}_{yy,r} = -\text{diag}\begin{bmatrix} 0 & 1 & 2^2 \cdots & S^2 \end{bmatrix}$$

The matrix $\mathbf{R}_{xy}$ is constituted by $(R + 1)$ matrices $\mathbf{R}_{xy,r}$,

$$\mathbf{R}_{xy} = \text{diag}\begin{bmatrix} \mathbf{R}_{xy,0} & \mathbf{R}_{xy,1} & \cdots & \mathbf{R}_{xy,R} \end{bmatrix}$$

The matrices $\mathbf{R}_{xy,r}$ are diagonal too and have $(S + 1)$ elements,

$$\mathbf{R}_{xy,r} = r \cdot \text{diag}\begin{bmatrix} 0 & 1 & 2 \cdots & S \end{bmatrix}$$

Analogous to (A10), using the same notations, the relations,

$$\mathbf{z}''_{xx} = \mathbf{T}_{xx} \cdot \mathbf{Z}''_{xx}\quad \mathbf{z}''_{yy} = \mathbf{T}_{yy} \cdot \mathbf{Z}''_{yy}\quad \text{and}\quad \mathbf{z}''_{xy} = \mathbf{T}_{xy} \cdot \mathbf{Z}''_{xy} \tag{A20}$$

can be created. The matrices $\mathbf{T}_{xx}$ and $\mathbf{T}_{yy}$ fulfill the relation $\mathbf{T}_{xx} = \mathbf{T}_{yy} = \mathbf{T}$ and the matrix $\mathbf{T}_{xy}$ can be easy predicted as,

$$\mathbf{T}_{xy} = \begin{bmatrix} \sin(0 \cdot x_1) \cdot \mathbf{B}_y & \sin(1 \cdot x_1) \cdot \mathbf{B}_y & \cdots & \sin(R \cdot x_1) \cdot \mathbf{B}_y \\ \sin(0 \cdot x_2) \cdot \mathbf{B}_y & \sin(1 \cdot x_2) \cdot \mathbf{B}_y & \cdots & \sin(R \cdot x_2) \cdot \mathbf{B}_y \\ \vdots & \vdots & \vdots & \vdots \\ \sin(0 \cdot x_{R+1}) \cdot \mathbf{B}_y & \sin(1 \cdot x_{R+1}) \cdot \mathbf{B}_y & \cdots & \sin(R \cdot x_{R+1}) \cdot \mathbf{B}_y \end{bmatrix} \tag{A21}$$

The mathematical operations described below,

$$(\mathbf{T} \cdot \mathbf{Z}''_{xx}) = \left(\mathbf{T} \cdot \mathbf{R}_{xx} \cdot \mathbf{T}^{-1}\right) \cdot (\mathbf{T} \cdot \mathbf{Z})$$
$$\left(\mathbf{T} \cdot \mathbf{Z}''_{yy}\right) = \left(\mathbf{T} \cdot \mathbf{R}_{yy} \cdot \mathbf{T}^{-1}\right) \cdot (\mathbf{T} \cdot \mathbf{Z})$$
$$\left(\mathbf{T}_{xy} \cdot \mathbf{Z}''_{xy}\right) = \left(\mathbf{T}_{xy} \cdot \mathbf{R}_y \cdot \mathbf{T}^{-1}\right) \cdot (\mathbf{T} \cdot \mathbf{Z})$$

lead to relations defining the second order partial differential operators,

$$\mathbf{z}''_{xx} = \mathbf{D}^{(2)}_{xx} \cdot \mathbf{z}\quad \mathbf{z}''_{yy} = \mathbf{D}^{(2)}_{yy} \cdot \mathbf{z}\quad \mathbf{z}''_{xy} = \mathbf{D}^{(2)}_{xy} \cdot \mathbf{z} \tag{A22}$$

where

$$\mathbf{D}_{xx}^{(2)} = \mathbf{T} \cdot \mathbf{R}_{xx}^{(2)} \cdot \mathbf{T}^{T} \; ; \; \mathbf{D}_{yy}^{(2)} = \mathbf{T} \cdot \mathbf{R}_{yy}^{(2)} \cdot \mathbf{T}^{T} \; ; \; \mathbf{D}_{xy}^{(2)} = \mathbf{T}_{xy} \cdot \mathbf{R}_{xy}^{(2)} \cdot \mathbf{T}^{T} \tag{A23}$$

where

$$\mathbf{R}_{xx}^{(2)} = \mathbf{R}_{xx} \cdot \mathbf{C}^{-1} = \frac{1}{(R+1)\cdot(S+1)} \text{diag} \begin{bmatrix} 0 & 2 \cdot \mathbf{R}_{xx,1}^{(2)} & \cdots & 2 \cdot \mathbf{R}_{xx,R}^{(2)} \end{bmatrix}$$

$$\mathbf{R}_{xx,r}^{(2)} = -r^2 \cdot \text{diag} \begin{bmatrix} 1 & 2 & \cdots & 2 \end{bmatrix}$$

$$\mathbf{R}_{yy}^{(2)} = \mathbf{R}_{yy} \cdot \mathbf{C}^{-1} = \frac{1}{(R+1)\cdot(S+1)} \text{diag} \begin{bmatrix} \mathbf{R}_{yy,S}^{(2)} & 2 \cdot \mathbf{R}_{yy,S}^{(2)} & \cdots & 2 \cdot \mathbf{R}_{yy,S}^{(2)} \end{bmatrix}$$

$$\mathbf{R}_{yy,S}^{(2)} = -2 \cdot \text{diag} \begin{bmatrix} 0 & 1^2 & \cdots & S^2 \end{bmatrix}$$

$$\mathbf{R}_{xy}^{(2)} = \mathbf{R}_{yy} \cdot \mathbf{C}^{-1} = \frac{1}{(R+1)\cdot(S+1)} \text{diag} \begin{bmatrix} 0 & 2 \cdot \mathbf{R}_{xy,1}^{(2)} & \cdots & 2 \cdot \mathbf{R}_{xy,R}^{(2)} \end{bmatrix} \mathbf{R}_{xy,r}^{(2)} = 2 \cdot r \cdot \text{diag} \begin{bmatrix} 0 & 1 & \cdots & S \end{bmatrix}$$

The matrices $\mathbf{R}_{xx}^{(2)}$, $\mathbf{R}_{yy}^{(2)}$ and $\mathbf{R}_{yx}^{(2)}$ are singular.

References

1. Arnold, E.; la Cour, J.L. *Die Transformatoren*; Springer: Berlin, Germany, 1910.
2. Richter, R. *Elektrische Maschinen, Bd.3, Die Transformatoren*; Birkhäuser: Basel, Switzerland, 1954.
3. Jezierski, E. *Transformers, Theoretical Background*; Wydawnictwa Naukowo-Techniczne (WNT): Warsaw, Poland, 1965. (In Polish)
4. Karsai, K.; Kerenyi, D.; Kiss, L. *Large Power Transformers*; Elsevier Publications: Amsterdam, The Netherlands, 1987.
5. Winders, J.J., Jr. *Power Transformers, Principles and Applications*; Pub. Marcel Dekker Inc.: New York, NY, USA, 2002.
6. Del Vecchio, R.M.; Poulin, B.; Feghali, P.T.; Shah, D.M.; Ahuja, R. *Transformers Design and Principles with Applications to Core-Form Power Transformers*; Taylor & Francis: New York, NY, USA, 2002.
7. Hurley, W.G.; Wölfle, W.H. *Transformers and Inductors for Power Electronics: Theory, Design & Applications*; John Wiley & Sons Pub.: Hoboken, NJ, USA, 2013.
8. Chiver, O.; Neamt, L.; Horgos, M. Finite elements analysis of a shell-type transformer. *J. Electr. Electron. Eng.* **2011**, *4*, 21.
9. Tsili, M.; Dikaiakos, C.; Kladas, A.; Georgilakis, P.; Souflaris, A.; Pitsilis, C.; Bakopoulos, J.; Paparigas, D. Advanced 3D numerical methods for power transformer analysis and design. In Proceedings of the 3rd Mediterranean Conference and Exhibition on Power Generation, Transmission, Distribution and Energy Conversion, MEDPOWER 2002, Athens, Greece, 4–6 November 2002.
10. Stanculescu, M.; Maricaru, M.; Hnil, F.I.; Marinescu, S.; Bandici, L. An iterative finite element-boundary element method for efficient magnetic field computation in transformers. *Rev. Roum. Sci. Technol.* **2011**, *56*, 267–276.
11. Jamali, S.; Ardebili, M.; Abbaszadeh, K. Calculation of short circuit reactance and electromagnetic forces in three phase transformers by finite element method. In Proceedings of the 8th International Conference Electrical Machines & Systems, Nanjing, China, 27–29 September 2005; Volume 3, pp. 1725–1730.
12. Hameed, K.R. Finite element calculation of leakage reactance in distribution transformer wound core type using energy method. *J. Eng. Dev.* **2012**, *16*, 297–320.
13. Oliveira, L.M.R.; Cardoso, A.J.M. Leakage inductances calculation for power transformers interturn fault studies. *IEEE Trans. Power Deliv.* **2015**, *30*, 1213–1220. [CrossRef]
14. Kaur, T.; Kaur, R. Modeling and computation of magnetic leakage field in transformer using special finite elements. *Int. J. Electron. Electr. Eng.* **2016**, *4*, 231–234. [CrossRef]
15. Ehsanifar, A.; Dehghani, M.; Allahbakhshi, M. Calculating the leakage inductance for transformer inter-turn fault detection using finite element method. In Proceedings of the 2017 Iranian Conference on Electrical Engineering (ICEE), Tehran, Iran, 2–4 May 2017. [CrossRef]

16.   Caron, G.; Henneron, T.; Piriou, F.; Mipo, J.-C. Waveform relaxation-Newton method to determine steady state operation: Application to three-phase transformer. *COMPEL Int. J. Comput. Math. Electr. Electron. Eng.* **2017**, *36*, 729–740. [CrossRef]

17.   Guemes-Alonso, J.A. A new method for calculating of leakage reactances and iron losses in transformers. In Proceedings of the Fifth International Conference on Electrical Machines and Systems (IEEE Cat. No.01EX501), Shenyang, China, 18–20 August 2001; Volume 1, pp. 178–181. [CrossRef]

18.   Schlesinger, R.; Biela, J. Comparison of analytical models of transformer leakage inductance: Accuracy versus computational effort. *IEEE Trans. Power Electron.* **2002**, *36*, 146–156. [CrossRef]

19.   Jahromi, A.; Faiz, J.; Mohseni, H. A fast method for calculation of transformers leakage reactance using energy technique. *IJE Trans. B Appl.* **2003**, *16*, 41–48.

20.   Jahromi, A.; Faiz, J.; Mohseni, H. Calculation of distribution transformer leakage reactance using energy technique. *J. Fac. Eng.* **2004**, *38*, 395–403.

21.   Dawood, K.; Alboyaci, B.; Cinar, M.A.; Sonmez, O. A new method for the calculation of leakage reactance in power transformers. *J. Electr. Eng. Technol.* **2017**, *12*, 1883–1890. [CrossRef]

22.   Dawood, K.; Cinar, M.A.; Alboyaci, B.; Sonmez, O. Calculation of the leakage reactance in distribution transformers via numerical and analytical methods. *J. Electr. Syst.* **2019**, *15*, 213–221.

23.   Sobczyk, T.; Jaraczewski, M. On simplified calculations of leakage inductances of power transformers. *Energies* **2020**, *13*, 4952. [CrossRef]

24.   Wachta, B. Calculation of leakages in unsymmetrical multi-windings transformers. *Sci. Bull. Univ. Min. Metall. Kraków Pol.* **1969**, *243*, 7–27. (In Polish)

25.   Sobczyk, T.J.; Jaraczewski, M. Application of Discrete Differential Operators of Periodic Function to Solve 1D Boundary Value Problems. *COMPEL Int. J. Comput. Math. Electr. Electron. Eng.* **2020**, *39*, 885–897. [CrossRef]

26.   Sobczyk, T.J. 2D discrete operators for periodic functions. In Proceedings of the 2019 15th Selected Issues of Electrical Engineering and Electronics (WZEE), Zakopane, Poland, 8–10 December 2019; ID12, IEEE Explore: 978-1-7281-1038-7/19.